Neuronal SNAREs Do Not Trigger Fusion between Synthetic Membranes but Do Promote PEG-Mediated Membrane Fusion

S. Moses Dennison,* Mark E. Bowen,[†] Axel T. Brunger,[†] and Barry R. Lentz*

*Department of Biochemistry and Program in Molecular/Cell Biophysics, University of North Carolina, Chapel Hill, North Carolina 27599; and [†]Howard Hughes Medical Institute and Departments of Molecular and Cellular Physiology, Neurology, and Neurological Sciences and Stanford Synchrotron Radiation Laboratory, Stanford University, Stanford, California 94305

ABSTRACT   At low surface concentrations that permit formation of impermeable membranes, neuronal soluble *N*-ethyl maleimide sensitive factor attachment protein receptor (SNARE) proteins form a stable, parallel, *trans* complex when vesicles are brought into contact by a low concentration of poly(ethylene glycol) (PEG). Surprisingly, formation of a stable SNARE complex does not trigger fusion under these conditions. However, neuronal SNAREs do promote fusion at low protein/lipid ratios when triggered by higher concentrations of PEG. Promotion of PEG-triggered fusion required phosphatidylserine and depended only on the surface concentration of SNAREs and not on the formation of a *trans* SNARE complex. These results were obtained at protein surface concentrations reported for synaptobrevin in synaptic vesicles and with an optimally fusogenic lipid composition. At a much higher protein/lipid ratio, vesicles joined by SNARE complex slowly mixed lipids at 37°C in the absence of PEG, in agreement with earlier reports. However, vesicles containing syntaxin at a high protein/lipid ratio ($\geq$1:250) lost membrane integrity. We conclude that the neuronal SNARE complex promotes fusion by joining membranes and that the individual proteins syntaxin and synaptobrevin disrupt membranes so as to favor formation of a stalk complex and to promote conversion of the stalk to a fusion pore. These effects are similar to the effects of viral fusion peptides and transmembrane domains, but they are not sufficient by themselves to produce fusion in our in vitro system at surface concentrations documented to occur in synaptic vesicles. Thus, it is likely that proteins or factors other than the SNARE complex must trigger fusion in vivo.

INTRODUCTION

Neuronal exocytosis requires docking of synaptic vesicles with the presynaptic plasma membrane and the subsequent fusion of two lipid bilayers. The three soluble *N*-ethyl maleimide sensitive factor attachment protein receptor (SNARE) proteins synaptobrevin (SB), located in the synaptic vesicle membrane, and syntaxin (SX) and SNAP-25 (SN25), both located in the presynaptic membrane, play an important role in this highly regulated process (1). The crucial role of the SNARE proteins in exocytosis is demonstrated by the sensitivity of transmitter release to clostridial neurotoxins, which specifically proteolyze SNAREs, along with several studies showing that mutations or factors affecting SNARE complex formation blocked release (summarized in Chen and Scheller (2)).

Although the importance of SNAREs for synaptic vesicle release is widely accepted, the molecular mechanism by which SNAREs might participate in fusion remains unresolved. Membrane fusion is generally viewed as a multistep process (3). To determine how SNARE proteins influence the fusion reaction, one needs kinetic data on lipid mixing, contents mixing, and contents leakage in the presence and absence of SNARE complex. To date, studies examining the effects of SNAREs on fusion have not monitored all these parameters. We reconstituted SNARE proteins into small unilamellar vesicles (SUVs) with a lipid composition similar to that of synaptic vesicles, which were optimally fusogenic

(4), at protein/lipid (P/L) ratios of 1:2250 and 1:950 for SX and SB, respectively. Detergent-assisted incorporation of SNARE proteins into preformed vesicles at low P/L ratios produced impermeable vesicles capable of retaining soluble contents, which allowed contents mixing during fusion to be studied and resulted in an asymmetric orientation of SNAREs such that all cytosolic domains faced outward.

At the low surface density of SNAREs used, the probability of forming a *trans* complex during a vesicle collision is small. To expedite complex formation, we used low concentrations (3 wt %) of poly(ethylene glycol) (PEG) to aggregate the vesicles. Under these conditions, vesicle phosphate groups are separated by 15–20 Å, but adjacent bilayers do not fuse (4,5). Once we verified formation of *trans* SNARE complexes after diluting the PEG to less than aggregating concentration, we sought to answer several questions related to the role of SNARE complex in fusion. Does intervesicle SNARE complex formation result in spontaneous fusion of vesicles? If not, do the SNARE complex or SNARE proteins affect the rate or extent of fusion induced by PEG? If so, which step(s) of PEG mediated fusion is/are affected by the SNARE complex and why? We found that the neuronal SNARE complex was sufficient to dock SUVs but did not induce fusion. At PEG concentrations sufficient to induce fusion, we found that SNARE proteins enhanced fusion, but only in the presence of phosphatidylserine. The enhancement of fusion did not require SNARE complex formation, suggesting a similarity to the membrane-perturbing transmembrane domains and fusion peptides of viral

fusion proteins. Thus, the neuronal SNARE complex is not a complete fusion machine, at least at the low P/L ratios studied here.

MATERIALS AND METHODS

Recombinant proteins

Full-length cDNAs for rat SX-1A, SNAP-25A (SN25), and SB-II were expressed in *Escherichia coli*, and purified as described previously (6,7). Proteins were specifically labeled at cysteine residues introduced near the N-terminus of the SNARE motif after all endogenous cysteines were mutated to serine (S193C-SX, S28C-SB, and Q20C-SN25) (6). SX was labeled with fluorescein maleimide (Molecular Probes, Eugene, OR) (referred to as F-SX), and SB and SN25 were labeled with tetramethylrhod-amine maleimide (Molecular Probes) (referred to as R-SB and R-SN25) as described previously (6). The labeling sites were chosen so that probe molecules would be within 10–12 Å of each other when a parallel SNARE complex is assembled (6), giving maximal fluorescence resonance energy transfer (FRET) from fluorescein to rhodamine. SX labeled with fluorescein maleimide at a cysteine introduced at position 249 (Fa-SX) was also produced to check for antiparallel complex. Labeling efficiency was assessed by measuring absorbance at 492 nm for fluorescein ($\varepsilon = 83,000$ $M^{-1} cm^{-1}$) and at 541 nm for tetramethylrhodamine ($\varepsilon = 91,000 M^{-1} cm^{-1}$) and then dividing the calculated probe concentration by the protein concentration. Labeling efficiencies were 50–60% for F-SX, 40–55% for R-SB, and 68% for R-SN25.

Phospholipids and other reagents

Chloroform stock solutions of 1,2-dioleoyl-3-*sn*-phosphatidylcholine (DOPC), 1,2-dioleoyl-3-*sn*-phosphatidylethanolamine (DOPE), 1,2-dioleoyl-3-*sn*-phosphatidylserine (DOPS), bovine brain sphingomyelin (SM), cholesterol (CH), *N*-(7-nitro-2,1,3-benzoxadiazole-4-yl)-1,2-dipalimitoyl-3-*sn*-phosphatidylserine (NBD-PS), and *N*-(lissamine rhodamine B sulfonyl)-1,2-dipalmitoyl-3-*sn*-phosphatidylethanolamine (rhodamine-PE) were purchased from Avanti Polar Lipids (Alabaster, AL). All except CH were used without further purification. The concentrations of all the stock phospholipids were determined by a phosphate assay (8). CH was purified as reported (9). 2-(4,4-difluoro-5,7-diphenyl-4-bora-3a,4a-diaza-s-indacene-3-dodecanoyl)-1-hexadecanoyl-*sn*-glycero-3-phosphoethanolamine (BODIPY530-PE) and 2-(4,4-difluoro-5,7-diphenyl-4-bora-3a,4a-diaza-s-indacene-3-dodecanoyl)-1-hexadecanoyl-*sn*-glycero-3-phosphocholine (BODIPY500-PC) were from Molecular Probes. Terbium chloride was obtained from Johnson Matthey (Ward Hill, MA). *N*-[tris(hydroxymethyl)methyl]2-2-aminoethane sulphonic acid (TES) was purchased from Sigma Chemical (St. Louis, MO). PEG of molecular weight 7000–9000 (PEG 8000) was purchased from Fisher Scientific (Fairlane, NJ) and further purified as reported (10). Dodecyloctaethylene glycol monoether ($C_{12}E_8$), and dithiothreitol (DTT) were purchased from Calbiochem (La Jolla, CA). β-octyl-glucoside (β-OG) was obtained from Anatrace (Maumee, OH). C^{14}-labeled β-octyl-glucoside was obtained from American Radiolabeled Chemicals (St. Louis, MO). All other reagents were of the highest purity grade available.

Vesicle preparation and reconstitution of SNARE proteins

SUVs composed of DOPC/DOPE/SM/CH/DOPS (32:25:15:20:8 molar ratio) and DOPC/DOPE/SM/CH (35:30:15:20 molar ratio) were chosen for these studies for the following reasons. First, these compositions have previously been optimized for PEG-mediated fusion and roughly match the composition of synaptic vesicles (4). Second, SUVs of these compositions

have small diameters, making them highly curved. Curvature promotes fusion in vitro and likely plays the same role in vivo. It was our purpose to encourage fusion, making it most likely that SNARE complex would function to trigger fusion if it could. Vesicles were prepared as reported earlier (4). The mean diameter of the vesicles was measured by quasielastic laser light scattering (QELS) using a custom built multiangle photometer that incorporates a computing autocorrelator from Particle Sizing Systems (Santa Barbara, CA) (10). The vesicle size was calculated in the volume weighted mode using a Gaussian size distribution. Mean diameters were reproducibly in the range of 17–22 nm for DOPS-containing and 24–26 nm for DOPS-free vesicles.

SX (80 μM) and SB (190 μM) in 20 mM Tris, 200 mM NaCl, 1 mM DTT, and 100 mM β-OG, pH 8.0 buffer were mixed with vesicles that had been prepared appropriately for lipid mixing, contents mixing, or leakage assays (usually 40–45 mM lipid concentration) at a 1:4 ratio (v/v) and equilibrated at room temperature for ~1 h. For controls, protein-free buffer was added to vesicles. The protein vesicle mixtures and the control samples were placed in a dialysis tube (50,000 molecular weight cutoff) and dialyzed for 24 h (sample/buffer ratio 1:1000) with two buffer exchanges to remove detergent (Fig. 1). The dialysis buffer contained 20 mM Tris, 200 mM NaCl, 1 mM EDTA, and 1 mM DTT, pH 7.4. After dialysis, samples were removed from the dialysis bag, and the mean diameter of the vesicles was estimated. For double, triple, and quadruple reconstitutions, SX and SB vesicle samples after single, double, and triple reconstitutions were mixed with SX and SB, respectively, in detergent solution (4:1 ratio v/v) and dialyzed for another 24 h after an hour of equilibration at room temperature. We determined the size of the vesicles by quasielastic light scattering after each reconstitution to confirm that reconstitution had not perturbed vesicle integrity. The concentration of phospholipids in the vesicle samples was determined using DOPC that has been spiked with ^{14}C-labeled 1,2-dipalmitoyl-3-*sn*-phosphatidylcholine. A nonlipid-interfering protein assay (Geno Technology, St. Louis, MO) was used to estimate the concentration of proteins in the vesicle samples. The P/L ratio of the vesicle samples was close to the expected values based on starting protein and vesicle concentrations (1:2250 and 1:950 for SX and SB vesicles and ~1:980 and 1:420 for doubly reconstituted SX and SB vesicles). To determine the concentration of detergent remaining in the reconstituted vesicles, buffer (20 mM Tris, 200 mM NaCl, 1 mM DTT, and 100 mM β-OG) containing a trace amount of C^{14}-labeled β-OG and vesicles made from nonradio-labeled phospholipids were
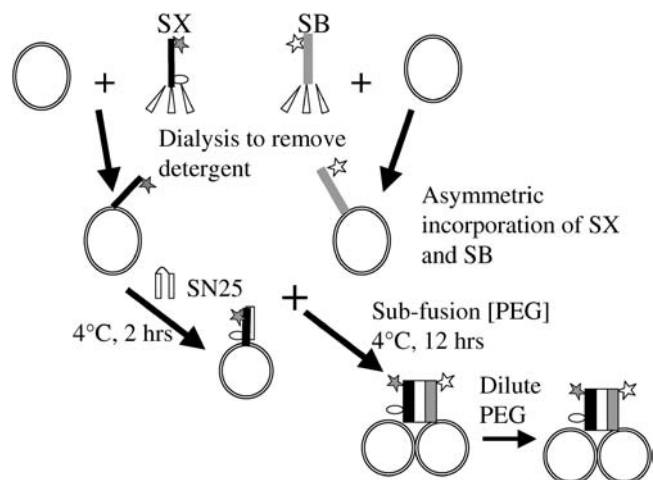

FIGURE 1 Cartoon summarizing the procedures leading to intervesicle SNARE complexes. Details are mentioned in Materials and Methods and Results. Solid and open stars indicate the positions of fluorescent probes fluorescein and tetramethylhodamine, respectively. The open circle indicates the label position of fluorescein in syntaxin (Fa-SX) used to detect antiparallel orientation of SX and SB.

used. Scintillation counting of samples before and after dialysis indicated that ~92% of added β-OG had been removed.

Assembly of the SNARE complex

SN25 was mixed with 100 μL of SX vesicles (final concentration: 28.5 μM for SN25, 20–23 mM total lipid, ~8 μM SX) and incubated for 2 h at 4°C. This incubation time was chosen based on FRET (see Fig. 3 *B, open diamonds*). The required amount of SB vesicles was then added to this mixture to maintain a 1:1 molar ratio of vesicles (on a lipid basis). The final concentration of SN25 in this mixture was ~15 μM, which was roughly twice the concentration of SX. PEG solution was added from a 30 wt % stock (w/v) to 150 μL of vesicles mixture, prepared as described above, to a final concentration of 3 wt % PEG. The PEG-treated vesicle mixtures were incubated at 4°C. Control experiments showed that this amount of PEG did not induce fusion or lipid mixing. A small aliquot (10 μL) of this incubation mixture was diluted at different times into 1 mL buffer for FRET and QELS measurements to judge the extent of complex assembly. To check the stability of the *trans* SNARE complexes, a small aliquot of the vesicle mixture incubated for over 12 h was diluted into 1 mL buffer, and FRET was monitored at regular intervals for ~8 h.

Contents-mixing, leakage, and lipid-mixing assays

The Tb^{3+}/dipicolinic acid (DPA) contents-mixing and leakage assays were based on those initially proposed by Wilschut et al. (11) and adapted to monitor PEG-induced fusion (12) and are described in detail in those publications. Vesicles prepared in Tb^{3+} or DPA buffer (for contents mixing) or Tb^{3+}/DPA buffer (for leakage) were used to make SX-, SB-, and protein-free control vesicles as described in the reconstitution procedure. Untrapped probe was removed during the dialysis step in the reconstitution of SNARE proteins. To measure contents mixing due to fusion, aliquots from SNARE vesicle assembly reactions were diluted into assay buffer equilibrated in a fluorescence cuvette at 23°C, and an appropriate amount of stock PEG solution (12 or 6 wt %) was added to produce final concentrations of 6 or 3 wt % PEG (for PS-containing and PS-free vesicles, respectively) and 0.2 mM total lipid. The increase in Tb^{3+} fluorescence was recorded with time, after which C$_{12}$E$_8$ was added to obtain the fluorescence of Tb^{3+}/DPA released from the vesicles as a reference. The percentage of contents mixing

was obtained by comparing the signal from the vesicle mixture with that of coencapsulated Tb/DPA vesicles, which was taken as indicative of 100% contents mixing (10). Leakage of contents was monitored with time by following the fluorescence of vesicles containing coencapsulated Tb^{3+}/DPA, with treatment with C$_{12}$E$_8$ used to mark 100% leakage of trapped contents (10). The contents-mixing signal was corrected for leakage (10).

The mixing of lipids was measured using the fluorescent lipid probes BODIPY500-PC and BODIPY530-PE (13). Vesicles containing both probes in a 1:1 molar ratio at 0.1 mol % each and probe-free vesicles were prepared. An increase in BODIPY500 signal indicates dilution of probes into probe-free vesicles. SX and SB vesicles and control vesicles were prepared as mentioned in reconstitution protocol. To more closely compare with results from other labs, some lipid-mixing experiments (see Fig. 7) were performed with NBD-PS and rhodamine-PE probes (1:1 molar ratio at 0.1 mol % each) instead of BODIPY probes.

For several reasons, the total percentage of contents mixing reported here is small. First, the endpoint of lipid mixing is always <100% due to the fact that lipid mixing and fusion occurs between vesicles in finite aggregates, with the endpoint of lipid mixing being a measure of mean aggregate size (14). Second, contents mixing and lipid mixing are measured on different scales, making lipid mixing always numerically greater than contents mixing. Because fusion does not always occur between a Tb^{3+} and a DPA vesicle, the scaling of the contents-mixing assay results in undercounting the number of fusion events. Third, lipid mixing registers a productive complex between vesicles, but only some productive complexes between vesicles result in fusion. Fusion was examined here at the threshold PEG concentration for which contents mixing is observed. This is because we wanted to limit leakage and maximize our ability to see an effect of SNARE complex. We showed previously that increasing concentrations of PEG lead to increasing contents mixing, presumably because more productive contacts convert to fusion pores and to increased leakage (15). High leakage leads to a decrease in contents mixing as most contents leak out (15).

Because the time course of complex assembly was much slower than that of PEG-mediated fusion, time courses of lipid mixing and contents mixing were collected on preassembled complexes for up to 500 s. These were fit to an empirical equation containing a single or the sum of two exponentials, as given in Table 1. The correlation coefficient and the *t*-test were relied on to judge the goodness of fit. For several samples, parameters obtained from the exponential analysis of 500-s time courses were compared with those from time courses collected intermittently (to avoid bleaching) for 1 h and were found to be essentially the same, indicating that 500 s were sufficient to

TABLE 1 Dependence of the kinetics of PEG- (6 wt %) induced fusion of small, unilamellar vesicles on the presence of reconstituted SX and SB and added SN25 and on formation of a *trans* SNARE complex between vesicles

Sample	Lipid mixing					Contents mixing				
	C_1 %	k_1 10^{-3} s^{-1}	C_2 %	k_2 10^{-3} s^{-1}	$C_1 + C_2$ %	C_1 %	k_1 10^{-3} s^{-1}	C_2 %	k_2 10^{-3} s^{-1}	$C_1 + C_2$ %
After single reconstitution of SX and SB										
Control			66.7 ± 0.4	3.7 ± 0.2	66.7 ± 0.4			3.7 ± 0.3	1.8 ± 0.2	3.7 ± 0.3
SX:SB complex			60.1 ± 0.3	4.0 ± 0.3	60.1 ± 0.3			3.8 ± 0.3	3.6 ± 0.6	3.8 ± 0.3
Control + SN25			70.9 ± 0.4	3.2 ± 0.1	70.9 ± 0.4			3.9 ± 0.4	1.9 ± 0.3	3.9 ± 0.4
SN25:SX:SB complex			64 ± 1	3.5 ± 0.2	64 ± 1			4.1 ± 0.48	4.0 ± 0.5	4.1 ± 0.5
After double reconstitution of SX and SB										
Control + SN25			73.3 ± 0.3	3.5 ± 0.2	73.3 ± 0.3			4.0 ± 0.3	1.9 ± 0.3	4.0 ± 0.3
SX:SB complex	15.6 ± 0.3	12.4 ± 2.8	54.2 ± 0.4	3.0 ± 0.3	69.8 ± 0.4	1.2 ± 0.1	26.8 ± 3.6	3.4 ± 0.2	2.5 ± 0.2	4.6 ± 0.2
SN25:SX:SB complex	16.5 ± 0.5	13.4 ± 1.8	55.5 ± 0.3	3.2 ± 0.3	72.0 ± 0.4	1.4 ± 0.04	23.2 ± 2.2	3.7 ± 0.26	2.6 ± 0.3	5.1 ± 0.3
After double reconstitution of SX and single reconstitution of SB										
Control + SN25			73.3 ± 0.3	3.5 ± 0.2	73.3 ± 0.3			4.0 ± 0.1	1.9 ± 0.2	3.98 ± 0.06
SX:SB complex	13.8 ± 0.2	14.5 ± 3.2	49.6 ± 0.5	3.4 ± 0.2	63.4 ± 0.6	0.8 ± 0.1	25.5 ± 6.2	3.3 ± 0.1	2.6 ± 0.3	4.09 ± 0.16
SN25:SX:SB complex	15.6 ± 0.4	12.4 ± 1.6	54.2 ± 0.3	3.0 ± 0.3	69.8 ± 0.4	1.1 ± 0.1	19.7 ± 2.6	3.6 ± 0.1	2.6 ± 0.4	4.71 ± 0.12

Exponential constants (k_1 and k_2) and preexponential factors (C_1 and C_2) were obtained by fitting the time courses of lipid mixing and contents mixing to the expression, $C_1[1 - \exp(-k_1 t)] + C_2[1 - \exp(-k_2 t)]$. Data obtained for different experiments were normalized with respect to control, which is an average of three experiments. The vesicle lipid composition was DOPC/DOPE/SM/CH/DOPS at a 32:25:15:20:8 molar ratio.
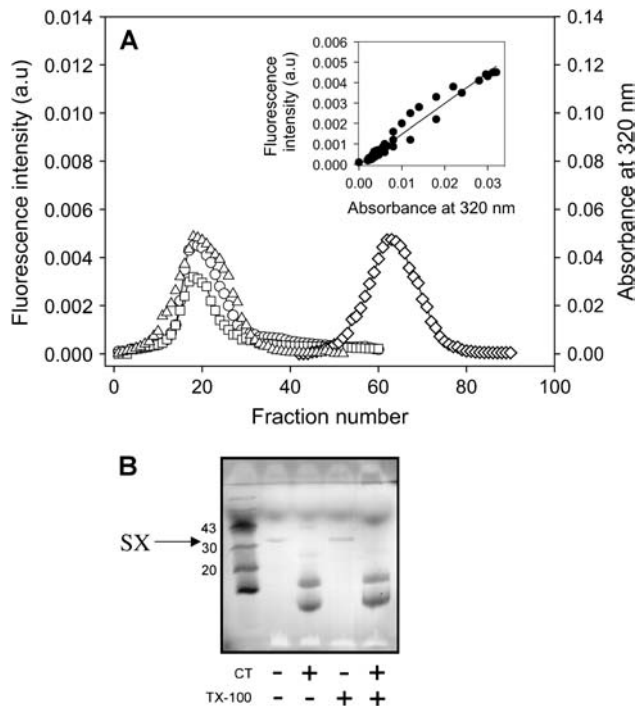
FIGURE 2 Demonstration of directed SX reconstitution into membrane vesicles. (A) Fluorescence (○) and turbidity (□) of F-SX vesicles, fluorescence of rhodamine-labeled SUV (△), and fluorescence of detergent-solubilized F-SX (◇) versus the fraction number collected from a Sepharose CL4B column. The inset shows a plot of fluorescence intensity of F-SX vesicles versus their turbidity. (B) SDS-PAGE of SX vesicles digested with CT before and after vesicle disruption by Triton X-100 (TX-100).

capture the exponential behavior and define the asymptotic extent of fusion or lipid mixing.

FRET measurements

FRET measurements were performed by diluting a small aliquot (10 μL) of PEG-treated vesicles mixture into a fluorescence cuvette containing 1 mL of 200 mM NaCl, 20 mM Tris, 1 mM DTT, pH 7.4 buffer. Fluorescence spectra were recorded from 490 nm to 650 nm while exciting fluorescein at 470 nm. Intensity at the fluorescein emission maximum (525 nm) for donor-only (F_D) and for donor-acceptor (F_{DA}) samples were recorded. At least three measurements were recorded for each sample to obtain $F_D/F_{DA} = R$.

RESULTS

Asymmetric reconstitution of syntaxin and synaptobrevin

The scheme for reconstitution of neuronal SNARE proteins into vesicles is shown in Fig. 1, with details of the procedure given in Materials and Methods. To verify whether fluorescein-labeled SX (F-SX) and rhodamine-labeled SB (R-SB) were efficiently reconstituted into vesicles, we passed the reconstituted vesicles through a Sepharose CL4B gel filtration column equilibrated with 200 mM NaCl, 20 mM Tris, 1 mM EDTA, and 1 mM DTT. The fluorescence intensities of detergent-solubilized F-SX (diamonds) and of F-SX vesicles

(circles) and the turbidity (absorbance at 320 nm; squares) of F-SX vesicles were recorded for each column fraction (Fig. 2 A). The turbidity and F-SX vesicle fluorescence profiles follow each other closely, as emphasized in the inset to Fig. 2 A, which correlates the fluorescence intensity of FSX vesicle fractions with the turbidity of the same fractions. Protein-free SUVs labeled with a rhodamine PE probe gave a similar elution profile to F-SX vesicles (triangles). Similar results were observed for R-SB vesicles (not shown). These results demonstrate that all detectable F-SX and R-SB were stably reconstituted into the vesicle fractions.

To determine the orientation of SNAREs in reconstituted vesicles, we treated SX and SB vesicles with chymotrypsin (CT) to proteolyze exposed SNAREs. The digested and undigested samples were analyzed by SDS-PAGE after heating the samples to 95°C in SDS-containing buffer. Fig. 2 B shows that SX samples digested by CT do not contain full-length SX, indicating that all detectable SX was cleaved by CT. Similar results were obtained for SB vesicles (data not shown). We conclude that SX and SB are asymmetrically incorporated into vesicles such that the cytoplasmic domains face the vesicle exterior.

Assembly and stability of the intervesicle SNARE complex

Because other groups have been unable to demonstrate mixing of contents, and thus fusion, between vesicles joined by SNARE complexes at high P/L ratios, we began by examining samples reconstituted at a low P/L ratio. Vesicles for these experiments resulted from a single reconstitution and contained SX at 1:2250 P/L and SB at 1:950 P/L. Since the surface concentrations of SX and SB are low in these samples, the probability of forming a trans complex during vesicle collisions is small. To expedite complex formation, we used low concentrations (3 wt %) of PEG to aggregate the vesicles and verified trans complex formation after diluting the PEG to a nonaggregating concentration (Fig. 1). The slow docking of SX vesicles precomplexed with SN25 (SN25:SX vesicles) with SB vesicles was detected using QELS to measure the mean diameter of the vesicles after dilution of PEG to a nonaggregating concentration (<0.1 wt %; solid circles, Fig. 3 A). Protein-free control vesicles (open circles), alone or in the presence of SN25 (open squares), increased only slightly in mean diameter in the same time period when incubated with the same amount of PEG. SNARE-containing vesicles incubated in the absence of PEG did not increase in mean diameter. These results indicate that SNARE proteins docked vesicles but only when the vesicles were juxtaposed by PEG. Control experiments showed that fluorescent labeling of SX or SB (representative data for SN25:Fa-SX vesicles and R-SB vesicles are shown as solid triangles in Fig. 3 A) did not interfere with docking. SX and SB vesicles docked as well as SN25:SX and SB vesicles, demonstrating that assembly of a SN25:SX binary complex is not necessary
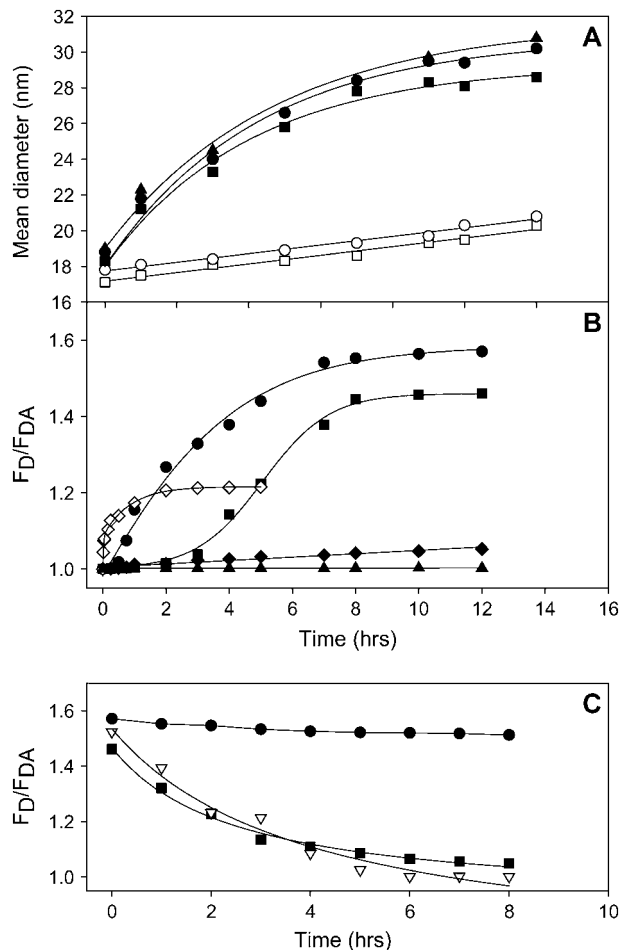
FIGURE 3 Time courses of SNARE complex assembly followed by light scattering and by FRET from fluorescein-labeled F-SX vesicles to tetramethylrhodamine-labeled R-SB vesicles. (A) Mean diameters of SN25:SX vesicles plus SB vesicles (●), SX vesicles plus SB vesicles (■), protein-free control vesicles (○), and control vesicles plus SN25 (□), SN25:Fa-SX vesicles plus R-SB vesicles (▲) as a function of incubation time with 3 wt % PEG. Before QELS measurements, vesicle samples were diluted to <0.1 wt % PEG (aggregation limit 1 wt %). (B) FRET (F_D/F_{DA}) for the same vesicle combinations and conditions described for frame A, with symbols as in frame A, with F-SX and R-SB replacing SX and SB. F_D/F_{DA} for SN25:F-SX vesicles plus R-SB vesicles when incubated without PEG is shown as solid diamonds. FRET from F-SX vesicles to R-SN25 (◇) shows the assembly of the SX/SN25 binary complex. FRET from SN25:Fa-SX vesicles to R-SB vesicles (▲) tests for assembly of antiparallel SNARE complex. (C) Stability of assembled SNARE complex (as detected by FRET efficiency) as a function of time after diluting PEG with symbols as in frame A and B except that the inverted open triangles show the disassembly of complex assembled from SX vesicles plus SB vesicles and SN25 without the preassembly of SX vesicles:SN25 complex.

to dock vesicles. This agrees with a study of docking of similarly reconstituted 50 nm SB vesicles to supported bilayers containing SX or SN25:SX (16). Additional control experiments showed that neither SX vesicles alone nor SB vesicles alone docked to themselves in the presence or absence of SN25 when incubated with 3% PEG (data not shown), suggesting that both SNAREs are needed for docking to occur.

To examine the relationship between vesicle docking and SNARE complex formation, we used interprotein FRET to monitor the assembly of SNARE proteins into a complex, comparable to an earlier report (17). The FRET time course was comparable to the QELS time course for vesicle-vesicle docking for a combination of SN25:SX vesicles with SB vesicles (Fig. 3 B, solid circles). However, formation of an SX-V:SB-V protein complex as detected by FRET (Fig. 3 B, solid squares) clearly shows a lag time as compared to the time course of vesicle-vesicle docking as judged by the mean vesicle diameter. This must mean that the SX and SB form a complex that joins vesicles but somehow is not mature enough to bring the FRET probes into close proximity. This profile also levels off at a lower FRET level than that seen for assembly of a SN25:SX-V:SB-V SNARE complex, suggesting that vesicles containing the binary SN25:SX complex form a somewhat different complex with SB vesicles than do SX vesicles. Association of SN25 with SX presumably avoids this structural maturing. We note that SX vesicles, SB vesicles, and SN25, when mixed simultaneously without preassembly of a SN25:SX complex, also form a SNARE complex, and without the delay seen for SX vesicles plus SB vesicles, but with a final FRET level intermediate between that of the SB vesicle:SX vesicle complex and the pre-assembled SN25:SX vesicle:SB vesicle complex (data not shown). The FRET signal for SN25:SX vesicles plus SB vesicles incubated without PEG did not increase significantly (solid diamonds in Fig. 3 B), indicating that it is very improbable at low P/L ratios that an intervesicle trans SNARE complex could assemble in the absence of PEG to force vesicle contact.

Complexes assembled in solution between cytoplasmic SX, SB, and SN25 constructs are quite stable and dissociate only upon boiling in SDS (18). We examined the stability of trans SNARE complexes formed between vesicles by diluting the docked vesicles to a PEG concentration well below that required to produce aggregation (<0.1 wt %) and monitoring FRET (Fig. 3 C). The complex formed between SX vesicles and SB vesicles dissociated completely within 8 h (solid squares). The complexes assembled in the presence of SN25 but without preassembly of a binary SN25:SX complex behaved similarly (open inverted triangles). However, the ternary complex assembled via a preassembled SN25:SX vesicle binary complex remained intact for the duration of our 8-h observation period (solid circles). Thus, preassembly a SN25:SX vesicle complex is required to form a stable trans SNARE complex, although vesicles can still be docked via a less stable SX vesicle:SB vesicle complex. Unless otherwise stated, we used the more stable complex for fusion experiments.

Characterization of the intervesicle SNARE complex

To characterize the extent and configuration of SNARE complex formed between vesicles, we needed to relate the

FRET measurements to formation of SNARE complex. To do this, we calibrated FRET measurements in solution, where formation of SNARE complex can be quantitated by SDS-PAGE. First, we titrated the F-SX:SN25 binary complex (1:2 ratio) with R-SB in β-OG and followed FRET. Fig. 4 shows a plot of the FRET R value (F_D/F_{DA}) versus the concentration of R-SB. The R value at saturation (R_{sat}) was 2, indicating a significant extent of FRET. We then performed the same titration using unlabeled full-length SX, SN25, and the cytosolic domain of SB and followed formation of SNARE complex after a 24-h incubation using SDS-PAGE (shown as *inset* to Fig. 4). Nearly all the SX present is incorporated into a SDS-resistant complex at SB/SX ratios >2:1. Since SX is the limiting component in this experiment, we equated SX incorporation with the extent of SNARE complex formation, and assumed that R_{sat} represents all SX being incorporated into SNARE complexes. Since this FRET signal reports only the parallel configuration of SNARE complex, we take R_{sat} as representative of parallel SNARE complex. We then used the titration curve (Fig. 4) to relate the FRET measurements to the extent of intervesicle complex formation, which yielded an estimate of ~80% SNARE complex formation ($R_{sat} \sim 1.6$) in vesicle samples. When we performed a double reconstitution (see Materials and Methods) to increase the SNARE content (P/L 1:980 and 1:420 for F-SX and R-SB vesicles), the complex assembled from these vesicles samples yielded only a slightly larger FRET R value (1.7), corresponding to ~85% complex
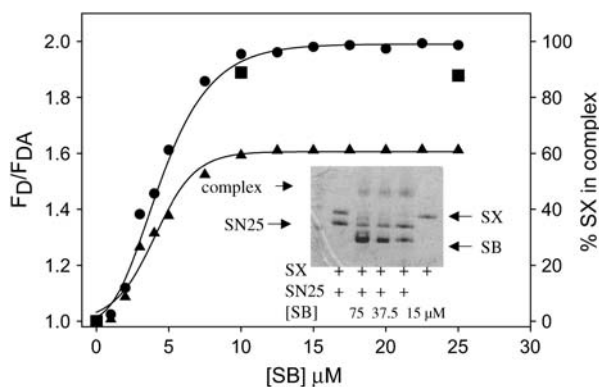

FIGURE 4 Estimation of complex assembly by FRET. (*A*) FRET (F_D/F_{DA}) from F-SX to R-SB (both β-OG solubilized) is plotted versus the concentration of R-SB added to a solution of F-SX:SN25 binary complex, with dye labels positioned to detect the parallel configuration (●) and the antiparallel configuration (▲) between SX and SB. A mixture of 5 μM F-SX and 10 μM SN25 was incubated for 30 min to produce F-SX:SN25 complex before adding varying amounts of R-SB and incubating for 24 h to form the full ternary complex. A small amount of this incubated mixture was diluted to 0.1 μM in F-SX for fluorescence measurements. The inset shows SDS-PAGE analysis without boiling samples of SNARE complex assembled from solubilized full-length SX (7.5 μM), SN25 (15 μM), and truncated SB (residues 1–96) after 24 h of incubation. Concentrations of SB were 2 and 5 times that of SX. Band intensities were digitized to calculate the percentage of SX in SNARE complex, and these values are shown as solid squares for comparison to the FRET values from labeled SNARE complex.

formation. Thus, *trans* SNARE complex formation in the presence of an aggregating concentration of PEG seems to be reasonably efficient and was not made significantly more efficient by doubling the SNARE content of vesicles.

Although the SNARE complex observed in the x-ray crystal structure has a parallel configuration (19), a small subpopulation of less stable antiparallel configurations have been reported when 50 nm-size unilamellar vesicles having reconstituted SB docked to planar-supported bilayers containing SX (6,16). To test for the existence of antiparallel configurations involved in docking vesicles held in contact by PEG, we assembled a complex in which SX was labeled with fluorescein at position 249 near its C-terminus (Fa-SX). In an antiparallel complex, this should be ~10–15 Å from rhodamine at position 28 of R-SB, leading to FRET. In solution, FRET was observed when this SNARE complex was assembled (Fa-SX:SN25:R-SB at a 1:2:5 ratio), indicating formation of some antiparallel complex (Fig. 4, *solid triangles*). Although 4–5% antiparallel complex was observed between SB vesicles and SX:SN25 incorporated into supported bilayers (16), no FRET was seen when SNARE complex was assembled from SN25:Fa-SX vesicles and R-SB vesicles held in contact by PEG (Fig. 3 *B*, *solid triangles*), even though light scattering indicated that intervesicle docking did occur (Fig. 3 *A*, *solid triangles*). It would appear that the balance between parallel and antiparallel SNARE complexes is influenced by the close juxtaposition of membranes containing the SNARE proteins and that only parallel complex formed under our conditions. Since the orientation of proteins in the SNARE complex in vivo has not been determined but the assembly of this complex in vivo is a complex process in which vesicles are actively juxtaposed to the target membrane (20), this observation implies that the SNARE complex formed in vivo may be the parallel complex.

Does SNARE complex formation trigger vesicle fusion?

We next considered the effect of SNARE complex on SUV fusion. After forming intervesicle SNARE complex in the presence of 3% PEG, PEG was diluted to a concentration well below that needed to produce aggregation (<0.1 wt %), almost no lipid mixing or contents mixing were observed for vesicles joined by *trans* SNARE complex at 23°C (*green dotted lines* in Fig. 5, *A* and *B*). To determine whether increased thermal energy might be needed for the SNARE complex to trigger, we tested for fusion at 37°C, a temperature at which others reported SNARE-mediated vesicle fusion (17,21–24). Slow lipid mixing did occur at 37°C, but control vesicles showed the same behavior (*inset* in Fig. 5 *A*). However, contents mixing was not observed at 37°C, either between vesicles joined by SNARE complex or between control vesicles (data not shown). Thus, *trans* complexes between SUVs reconstituted with neuronal SNAREs,
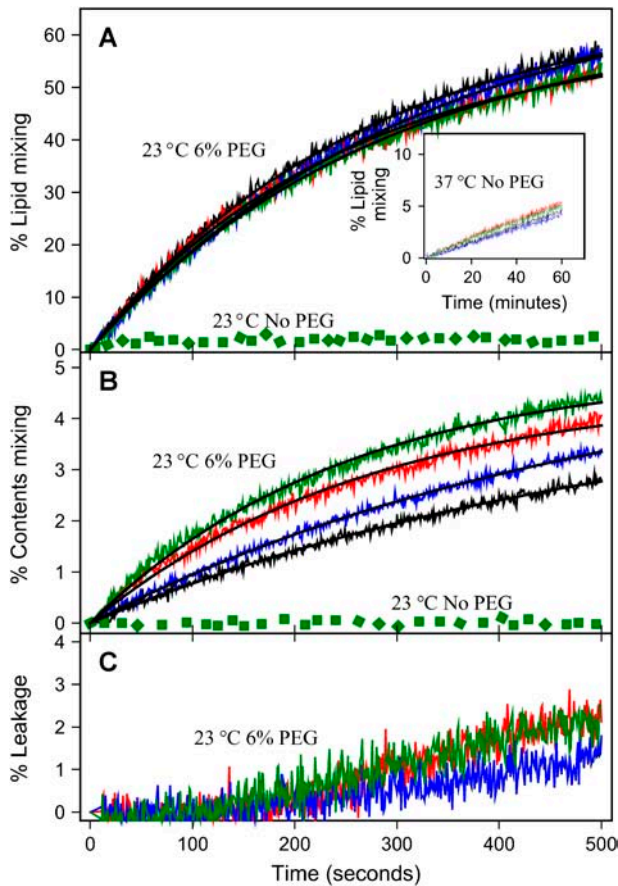
FIGURE 5   Effects of SNARE complexes on fusion. Time courses (at 23°C) of PEG- (6 wt %) induced (*A*) lipid mixing, (*B*) contents mixing, and (*C*) contents leakage of DOPC/DOPE/SM/CH/DOPS SUVs for protein-free control vesicles (*black*), SX-V:SB-V (*red*), control vesicles plus SN25 (*blue*), and SN25:SX-V:SB-V (*green*). Solid black lines through these time courses show the best fits of these time courses to single-exponential curves (see Materials and Methods). The invariant green dotted lines show time courses observed for SN25:SX-V:SB-V complexes at 23°C when no PEG was added to vesicles joined by stable SNARE complexes (SN25:SX-V:SB-V). The inset in frame *A* shows the time courses of lipid mixing for the same vesicle combinations described in frame *A* at 37°C when no PEG was present, conditions for which content mixing was not observed.

although quite stable, are not sufficient to induce fusion at either 23°C or 37°C, at least not at low P/L ratios.

Effect of SNARE complex on 6% PEG-mediated SUV fusion

Since the neuronal SNARE complex did not in itself induce fusion at either 23°C or 37°C, we asked next what effect the complex might have on PEG-mediated fusion. These experiments were carried out only at 23°C, since much of our previous work on PEG-mediated fusion was done at this temperature. At sufficiently high concentration, PEG induces fusion both by effecting close contact (5) and by exerting a compressive osmotic force (25). Fig. 5 *B* shows time courses of PEG-mediated fusion of control vesicles

(*black lines*), SB vesicle:SX vesicle complex (*red line*), and stable SB vesicle:SN25-SX vesicle complex (*green line*). These time courses were well described by a single exponential function that yielded an exponential constant and a preexponential factor (extent of fusion at infinite time) given in Table 1. These parameters reveal that the formation of *trans* SNARE complexes enhanced the rate of contents mixing by a factor of 2, whereas the extent of contents mixing was essentially unaffected. Vesicles joined by SB:SX complex behaved similarly to those joined by the stable SN25-SX:SB complex (Fig. 5, Table 1).

Surprisingly, the presence of SNARE proteins or *trans* SNARE complexes had a minimal effect on lipid mixing (Fig. 5 *A* and Table 1). This is because much more lipid mixing than contents mixing accompanies PEG-mediated fusion of vesicles. Lipid mixing is thus mainly a measure of productive contacts between vesicles in aggregates (26). Pore formation at a productive contact necessarily involves mixing of inner leaflet lipids, but these lipids constitute only ~1/3 of all the lipids in a 23 nm vesicle, and pores form at only a fraction of productive contacts (total contents mixing in most of our experiments was 4–5%, whereas total lipid mixing was 65–70%). Thus, the expected lipid mixing associated with pore formation would be ≤2%, not large enough to measure. SNAREs had no effect on vesicle leakage during the initial phase of PEG-mediated fusion but increased leakage rate slightly after an initial lag period (Fig. 5 *C*).

Recently, Bowen et al. (16) examined fusion of vesicles containing a low copy number of neuronal SNAREs and docked by these SNAREs to supported bilayers. They monitored fusion by release of the contents of single vesicles into the subbilayer space. In this case, fusion was also not induced by *trans* SNARE complex alone, but required laser-induced thermal heating as a trigger, in agreement with our observation that PEG is required to induce fusion.

Effect of SB/SX ratio

All experiments to this point have involved an SB/SX ratio of ~2, since this was the ratio at which SNARE complex formation was optimal in solution (Fig. 5 *A*). To determine how the SB/SX ratio influences intervesicular complex formation and fusion, we performed experiments with double-reconstituted SX vesicles (P/L 1:980) and single-reconstituted SB vesicles (P/L 1:950). FRET measurements indicated that SNARE complex formation was ~83% efficient, the same as observed between two double-reconstituted populations. Results of fusion experiments for these samples (Table 1) also were similar to results obtained with two double-reconstituted populations. It appears that a 1:1 ratio of SB/SX produced all the effects of a 2:1 ratio. Since doubling of SX without doubling of SB produced all the effects of doubling of both SX and SB surface concentrations, it seems that SX has a somewhat greater influence than SB on fusion.

Effect of SNARE surface concentration

Since most reports of SNARE-complex-mediated fusion used P/L ratios much higher than the 1:2250 (SX/L) and 1:950 (SB/L) ratios used in these experiments, we performed experiments with vesicles after single, double, triple, and quadruple reconstitution of SX (P/L ratios ~1:2250, 1:980, 1:460, and 1:250, respectively) and SB (P/L ratios ~1:950, 1:420, 1:260, and 1:120, respectively). SNARE complex was assembled by first assembling an SX vesicles:SN25 binary complex by incubating SX vesicles with SN25 at 4°C and then incubating this binary complex with SB vesicles (1:1 on lipid basis) over night at 4°C. Even at the higher SNARE P/L ratios of doubly reconstituted samples (1SX/980 and 1SB/420), the formation of neuronal SNARE complex did not induce lipid or contents mixing in the absence of PEG at 23°C (*green dots* in Fig. 6, *A* and *B*). At 37°C, lipid mixing (*inset* in Fig. 6 *A*) was comparable to that seen for singly reconstituted vesicles (*inset* in Fig. 5 *A*), and contents mixing again was not observed (data not shown).

When double-reconstituted vesicles were induced to fuse in the presence of 6 wt % PEG, the initial rate of lipid mixing increased slightly (Fig. 6 *A*). The total extent ($C_1 + C_2$) of lipid mixing was also not much increased by doubling the amount of SNAREs. However, the initial rate of contents mixing increased considerably (2.5-fold) relative to single-reconstituted vesicles. Visual inspection of the contents-mixing data (Fig. 6 *B*) easily reveals that the reason for the increase in initial rate is due to addition of a rapid initial increase. The time courses of both lipid mixing and contents mixing between doubly reconstituted-SNARE-linked vesicles were well described by a biexponential function (*solid lines* in Fig. 6), yielding the fast (component 1) and slow (component 2) exponential constants (k) and corresponding preexponential factors (C) presented in Table 1. This revealed that the effect of increased SNARE surface concentration was to introduce a fast component of contents mixing, whereas the long-time rate of contents mixing remained similar to that for the singly reconstituted sample (Table 1). The effect of increased SNARE content on leakage rate (Fig. 6 *C*) was also considerable (~2-fold increased after the initial lag period).

As a first step toward attempting fusion experiments at even higher surface concentrations of SNARE proteins, we checked whether vesicles retain their trapped contents after multiple reconstitution steps. Results obtained are presented in Fig. 7 *A*. Contents of the vesicles were retained without significant loss after single and double reconstitutions of both SB and SX. Triple reconstitution of SX led to significant loss of contents, and four reconstitutions with SX resulted in complete loss of contents (Fig. 7 *A*). Triple and quadruple reconstitutions of SB reduced trapped Tb^{3+} and DPA by ~20% but did not lead to a loss of membrane integrity. These results reveal why previous experiments in other labs failed to record contents mixing between SNARE-
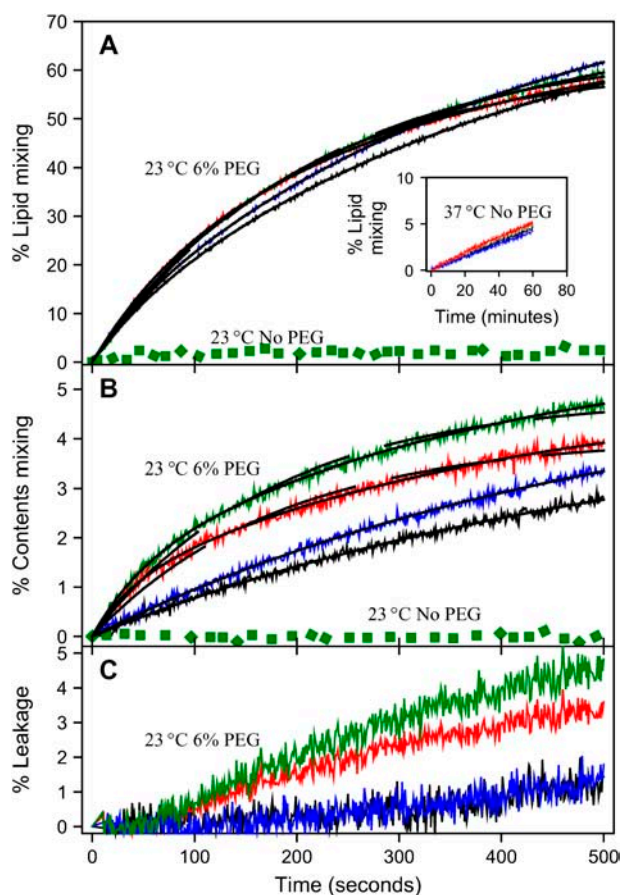
FIGURE 6 Effects of increased surface content of SNARE proteins. Time courses at 23°C of PEG- (6 wt %) mediated (*A*) lipid mixing, (*B*) contents mixing, and (*C*) contents leakage involving DOPC/DOPE/SM/CH/DOPS SUVs containing SX and SB at 1:980 and 1:420 protein/lipid ratios, respectively. Data are presented for protein-free control vesicles (*black lines*), SX-V:SB-V complexes (*red*), control vesicles plus SN25 (*blue lines*), and SN25:SX-V:SB-V complexes (*green lines*). Solid black lines on top of these time courses are the best fit obtained when these time courses were fit to a double-exponential expression. The dashed black lines in panels *A* and *B* show single-exponential fits for the time courses of SX-V:SB-V complexes (*red*) and SN25:SX-V:SB-V complexes (*green*). The invariant dotted green lines show time courses taken for SN25:SX-V:SB-V complexes at 23°C in the absence of PEG. The inset in frame *A* shows lipid-mixing kinetics for the same vesicle combinations described in frame *A* at 37°C in the absence of PEG, conditions for which content mixing was not observed.

complex-linked vesicles (17,21): SX (but not SB) at high surface concentration leads to loss of membrane integrity with respect to small solutes.

Next, we attempted to form SNARE complexes between vesicles in the absence of PEG, as described for singly reconstituted SN25:SX and SB vesicles. As for the singly and doubly reconstituted vesicles, we used QELS measurements of mean particle diameter as a quick check for SNARE complex formation. The mean diameter of quadruple-reconstituted SB (30 nm) vesicles was only slightly larger than those of control vesicles that underwent multiple detergent treatments without protein incorporation (24 nm),
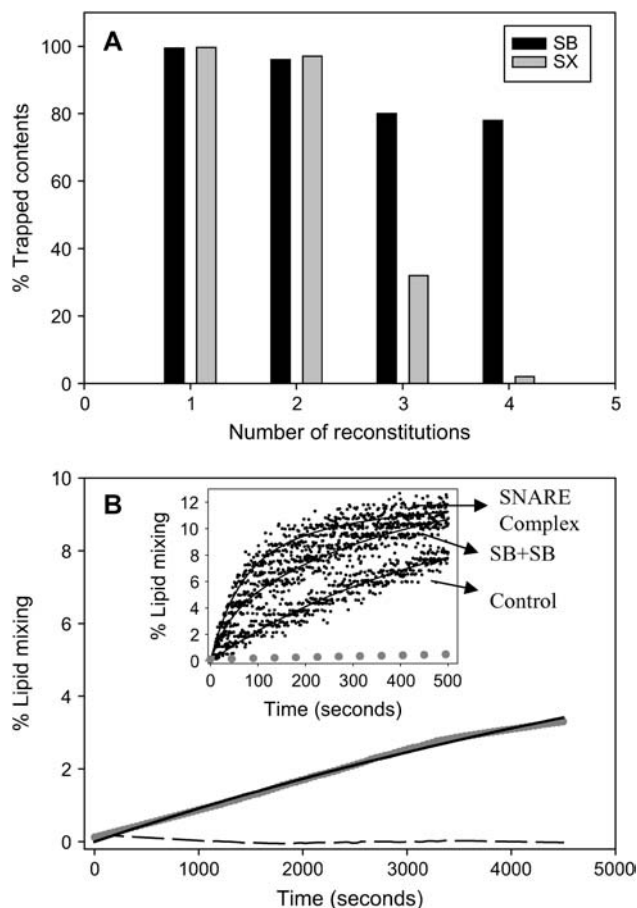
FIGURE 7 SNARE-induced lipid mixing and effect of SNARE reconstitution on loss of trapped contents. (A) Percentage of trapped contents of SX vesicles (gray bars) and SB vesicles (black bars) after single, double, triple, and quadruple reconstitutions. Percentage of trapped content was obtained from the difference in the intensities of Tb and DPA coencapsulated in vesicles before and after lysis using $C_{12}E_8$ detergent. These values were compared to those obtained for control vesicles at the respective reconstitution step to calculate percentage of trapped contents. (B) Lipid-mixing time courses of quadruple-reconstituted control vesicles (dashed line) and vesicles joined by stable SNARE complex (gray circles) incubated at 37°C in the absence of PEG. Samples incorporated SX and SB at P/L ratios of ~1:250 and 1:120, respectively. The inset shows time courses of lipid mixing at 23°C between control vesicles, vesicles joined by stable SNARE complex, and SB vesicles plus SB vesicles (all indicated by arrows), as triggered by 6% PEG. Gray dots show the data for SNARE-linked vesicles obtained in the absence of PEG, for reference. Solid black lines represent best fits of single (control in the inset and SNARE vesicles absent PEG at 37°C) or double exponentials to the data.

consistent with what we observed after single or double reconstitutions (Fig. 3 A). Quadruple-reconstituted SX vesicles increased more in size (40 nm). Unlike what we observed for singly and doubly reconstituted SN25:SX vesicles incubated with SB vesicles at 4°C in the absence of PEG, the mean diameter of mixtures of fourfold-reconstituted SB and SX:SN25 vesicles increased to 44 nm in 12 h. Freeze-fracture electron micrographs of this sample revealed small clusters of small vesicles, compared to control vesicles,

which were mainly single vesicles (J. M. Costello, S. M. Dennison, M. Temgire, and B. R. Lentz; unpublished observations). The mean diameter of quadruple-reconstituted vesicles treated with 3 wt % PEG at 4°C, to force aggregation and thus trigger intervesicle complex formation, was so large as to be beyond the dynamic range of our QELS system. Freeze-fracture electron micrographs of these samples showed large aggregates of many small and some larger vesicles (J. M. Costello, S. M. Dennison, M. Temgire, and B. R. Lentz; unpublished observations).

After assembling SNARE complex (in the absence of PEG) from quadruple-reconstituted SN25:SX and SB vesicles, this was diluted to 0.2 mM total lipid concentration in buffer equilibrated at 37°C and lipid mixing followed. Slow lipid mixing occurred as revealed by the increase in dequenching of NBD fluorescence (Fig. 7 B). Control vesicles or vesicles containing SNARE proteins without incubation to form a SNARE complex showed no increase in fluorescence. Because NBD-PS is less bright a fluorophore than our normal BODIPY500-PC lipid-mixing probe, the data were scattered and had to be smoothed by a running spline method. When fit to a single exponential (solid lines in Fig. 7 B), they revealed a rate constant of $1.1 \pm 0.1 \times 10^{-4}\%$ lipid mixing s^{-1} and a final extent of lipid mixing of 8.6% ± 0.4%. Unlike our lipid-mixing assay (13), the Rh-PE/NBD-PS results cannot be interpreted in terms of a calibration curve for local probe concentration. Instead, they must be referenced to a fluorescence intensity observed after detergent is added. This reference value depends on the details of the assay (probe concentration, probe-free versus probe-containing vesicle concentrations, detergent concentration). Thus, the rate obtained by this assay must be normalized by dividing by the asymptotic extent of lipid mixing to compare to results between labs. Doing so yields a rate of 0.13% of saturation s^{-1} for our results. Others using a similar assay (Rh-PE/NBD-PE with roughly equal concentrations of SB- and SN25:SX vesicles) obtained rates of 0.1% of saturation s^{-1} (21) and 0.14% of saturation s^{-1} (17). Thus, our results for mixing of lipids between SNARE-linked vesicles are completely consistent with those of previous researchers. QELS measurements showed that these vesicle samples increased in size to 50 nm in 75 min. Freeze-fracture electron microscopy showed a wide range of mainly single-walled vesicular structures in these samples (J. M. Costello, S. M. Dennison, M. Temgire, and B. R. Lentz; unpublished observations). Note that this behavior was unique to vesicles at high SNARE-protein content, as SNARE-linked, single- or double-reconstituted vesicles did not mix lipids or grow in size at 37°C to any extent greater than did protein-free control vesicles (Figs. 5 and 6 and results quoted above).

Clearly, we could not measure mixing of contents between these vesicles, as the SX vesicles had lost membrane integrity. Thus, to address these results to the issue of membrane fusion (''mixing of aqueous compartments without significant loss of contents''), we performed lipid-mixing experiments in the

presence of 6% PEG to trigger fusion. Not surprisingly, PEG trigger increased lipid mixing (Fig. 7 *B*, *inset*) between both control and SNARE-linked vesicles (indicated by *arrows*). The time dependence of lipid mixing between control vesicles was fit by a single exponential but required a double exponential for the SNARE-linked vesicles (Table 2). Comparison to Table 1 shows that the SNARE complex had the same effect on PEG-triggered lipid mixing at high protein content (1:120 and 1:250 SB and SX) as we observed for low protein content (1:420 and 1:980 SB and SX, double reconstitution in Table 1), where we were able to document that SNARE complex produced a fast component of contents mixing and thus promoted fusion. For comparison, we include in the inset the time course for lipid mixing in the absence of PEG but presence of the quadruple-reconstituted intervesicle SNARE complex (Fig. 7 *B*, *gray dots*). The initial rate of lipid mixing in the presence of PEG (1.5% of saturation s^{-1}) was roughly an order of magnitude greater than observed in the absence of PEG (0.13% of saturation s^{-1}).

Is a SNARE complex needed to observe enhanced fusion?

We asked next whether the fast lipid-mixing and contents-mixing component seen in doubly reconstituted vesicles might be due to closer apposition of vesicles joined by an increased surface density of *trans*-complex or simply due to higher protein contents in the vesicles. To answer this question, we used 6% PEG to induce fusion between 1), doubly reconstituted SX vesicles with SB vesicles mixed together but not given time to form a *trans* complex, 2), SB vesicles and SX vesicles incorporated into unstable *trans* complex, and 3), SB vesicles and SX vesicles after they have been given time to dissociate from an unstable *trans* complex. The fast component of lipid mixing was present in PEG-mediated fusion of all of these samples (Table 2), all of which had comparable total extents of lipid mixing. When we monitored PEG-triggered fusion between double-reconstituted SX vesicles and double-SX vesicles, a fast component of contents mixing was also seen (Table 3), along with increased contents leakage. The same behavior was seen for SN25:SX:SB-linked doubly reconstituted vesicles (Table 1),

for which it is clear that the fast component of contents mixing occurs at a rate similar to that of the fast component of lipid mixing. Double-reconstituted SB vesicles (Table 3) and quadruple-reconstituted SB vesicles (Table 2) behaved in a similar fashion. Neither SB plus SB vesicles nor SX plus SX vesicles formed intervesicle complexes, as judged by light scattering (data not shown). Finally, fusion of vesicles in the presence of SN25 alone (*blue lines* in Figs. 5 and 6) was almost indistinguishable from fusion of control vesicles (*black lines* in Figs. 5 and 6). These results demonstrate that it is higher surface concentrations of membrane-inserted SX and SB within vesicles, and not formation of more SNARE complex between vesicles, that result in a rapid component of fusion. Apparently, SX and SB promote fusion, but a SNARE complex between vesicles is not needed to see this fusion enhancement.

Effect of PS on fusion between SNARE-linked vesicles

Since PS is present in synaptic vesicles and in the plasma membrane with which they fuse (27) and because PS was reported to be necessary for Ca^{2+}-dependent SNARE-mediated fusion in the presence of synaptotagmin (24), we investigated the effect of PS in our reconstituted system. Thus, we reconstituted SNARE proteins into PS-free SUVs and assembled *trans* SNARE complexes in the same way as for PS-containing vesicles except that only 2% PEG was needed to aggregate these uncharged vesicles. FRET and light scattering both showed *trans* SNARE complex formation, although complex formation was reduced compared to that seen in the presence of PS (66% vs. 80% by FRET). As we observed for PS-containing vesicles, neuronal *trans* SNARE complex assembly did not induce either lipid mixing or contents mixing (data not shown). When the vesicles were induced to fuse by 3 wt % PEG (PS-free vesicles aggregate and fuse at lower concentrations of PEG (4)), we found that neuronal SNARE complex formation actually reduced the extent of contents mixing for vesicles lacking PS without affecting lipid mixing (Fig. 8 and Table 4). The time courses of lipid mixing and contents mixing were well described by a

TABLE 2 Dependence of PEG- (6 wt %) induced lipid mixing* of N-times reconstituted SX and SB vesicles in the presence or absence of a *trans* SNARE complex

Condition	N	C_1 %	k_1 10^{-3} s^{-1}	C_2 %	k_2 10^{-3} s^{-1}	$C_1 + C_2$ %
Control vesicles	2			73.3 ± 0.3	3.5 ± 0.2	73.3 ± 0.3
Not complexed	2	14.8 ± 0.4	13 ± 3	53.8 ± 0.6	3.1 ± 0.4	68.6 ± 0.4
Intact complex	2	15.6 ± 0.3	12 ± 3	54.2 ± 0.4	3.0 ± 0.3	69.8 ± 0.4
Dissociated complex	2	15.3 ± 0.3	12 ± 3	52.5 ± 0.5	3.2 ± 0.4	67.8 ± 0.5
Control vesicles	4			12.3 ± 0.5	2.0 ± 0.1	12.3 ± 0.5*
SNARE-complexed	4	7 ± 2	18 ± 4	5 ± 1.5	4 ± 2.5	12 ± 3.5*
SB and SB vesicles	4	2.9 ± 0.7	26 ± 0.1	10.4 ± 0.5	2.7 ± 0.7	13.3 ± 1.2*

*Total lipid mixing cannot be compared to that for the doubly reconstituted samples, since lipid mixing for the four-times-reconstituted samples was determined by the Rh-PE/NBD-PE assay, which determines total lipid mixing by addition of detergent at the end of the assay rather than by a calibration curve prepared from vesicles of known composition, as we do in our assay.

TABLE 3 Characteristics of the kinetics of PEG- (6 wt %) induced contents mixing of vesicles having the same SNARE proteins

Sample	C_1 %	k_1 10^{-3} s^{-1}	C_2 %	k_2 10^{-3} s^{-1}	$C_1 + C_2$ %
After single reconstitution					
SX + SX			4.12 ± 0.38	3.3 ± 0.3	4.12 ± 0.38
SB + SB			4.0 ± 0.4	3.2 ± 0.3	4.0 ± 0.4
After double reconstitution					
SX + SX	1.2 ± 0.2	18 ± 3	3.2 ± 0.2	2.3 ± 0.4	4.4 ± 0.2
SB + SB	1.3 ± 0.2	20 ± 3	3.2 ± 0.1	2.4 ± 0.3	4.4 ± 0.2

TABLE 4 Characteristics of the kinetics of PEG- (3 wt %) induced fusion of SNARE-containing but PS-free vesicles (single reconstitution)

	Lipid mixing		Contents mixing	
	C_2 %	k_2 10^{-3} S^{-1}	C_2 %	k_2 10^{-3} S^{-1}
Control	40.9 ± 0.5	2.3 ± 0.3	6.1 ± 0.6	2.0 ± 0.1
SX:SB complex	39.4 ± 0.5	2.7 ± 0.2	3.2 ± 0.4	1.6 ± 0.1
Control + SN25	40.6 ± 1.1	2.4 ± 0.1	5.1 ± 0.6	2.1 ± 0.1
SN25:SX:SB complex	38.8 ± 0.2	2.9 ± 0.3	4.7 ± 0.6	0.8 ± 0.1

single exponential function. Whereas a stably reconstituted *trans* SNARE complex decreased the rate of contents mixing by more than twofold relative to the control, the SX:SB complex lacking SN25 had little effect. We conclude that PS alters the interaction of SNARE proteins with membranes so that these proteins promote rather than inhibit fusion.
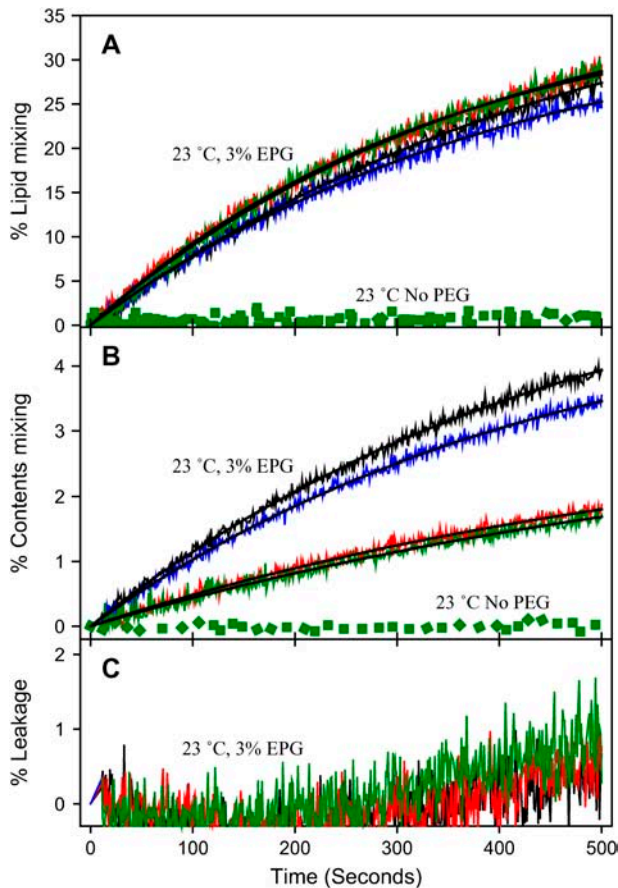
FIGURE 8 Effect of PS on SNARE effects on fusion. Time courses of (*A*) lipid mixing, (*B*) contents mixing, and (*C*) contents leakage involving DOPC/DOPE/SM/CH SUVs at 3 wt % PEG for protein-free control vesicles (*black*), SX vesicles plus SB vesicles (*red*), control vesicles plus SN25 (*blue*), and SN25/SX vesicles plus SB vesicles (*green*) with best fit shown as solid black lines. The green dotted lines show the time courses when no PEG was added to SN25/SX vesicles plus SB vesicles.

DISCUSSION

The reconstituted neuronal SNARE complex has been reported to be sufficient to induce lipid mixing in vitro, thus implying that it triggers fusion (21). An independent report with similarly reconstituted SNARE proteins showed in addition that SNARE complex formation induces a shift in the size distribution of vesicle-like structures (17). Schuette and co-workers (17) also demonstrated FRET between SX and SB labeled in the C-terminal regions and argued that this implied that SNARE complex triggers fusion. Although these observations do imply membrane merger, they do not demonstrate the SNARE-complex-induced mixing of trapped contents that could be taken as clear evidence of SNARE-triggered fusion. Nonetheless, these results have been interpreted to mean that the SNARE complex is the ''minimal machinery for cell membrane fusion'' (21). These experiments were done at a high P/L ratio ($\geq$1:100), so disruption and reannealing of contacting membranes could account for these results in the absence of true fusion. Indeed, there are many reports of phospholipid phase changes or membrane rupture caused by peptides, proteins, pH, or multivalent cations, etc. that result in lipid mixing but do not result in the joining of two aqueous compartments and thus do not qualify as fusion. Therefore, it remains unclear whether the assembled *trans* SNARE complex is a fusion machine in vitro although it contributes to efficient and rapid fusion in vivo (28).

Nonetheless, it is valid to ask what the mechanism is by which the SNARE complex contributes to membrane merger in vitro and whether this mechanism defines its role in vivo. In trying to answer these questions, we have shown that

1. SX and SB can be incorporated into preformed lipid vesicles in a fully directed fashion with nearly 100% efficiency and at a wide range of surface concentrations. The previous method for reconstitution of these proteins has led to incorporation at 65–80% efficiency and in a randomly directed fashion (17,21–24,29).
2. Reconstituted SX vesicles lose their membrane integrity at a P/L ratio of between 1:460 and 1:250, whereas SB vesicles retain their integrity vis-a-vis small solutes up to a 1:120 P/L ratio.
3. Reconstituted SX or SN25:SX complex assembles with reconstituted SB to form a parallel intervesicle SNARE

complex at ~85% efficiency, even at a very low copy number per vesicle, when vesicles are brought into contact with 3% PEG. The vesicle-SX:SN25:SB-vesicle complex is stable; the vesicle-SX:SB-vesicle complex is not. Thus, although SN25 is not needed to form an intervesicle SNARE complex, it is needed to form a stable membrane-joining complex.

4. Intervesicle SNARE complexes at very low surface concentration (SX/lipid and SB/lipid ratios of 1:2250 and 1:950) did not trigger fusion, but did increase the rate (but not extent) of pore formation between vesicles treated with 6% PEG to trigger fusion.

5. The membrane-inserted SNARE proteins (SX and SB) at intermediate concentration (1:980 for SX and 1:420 or 1:980 for SB) still could not trigger fusion but promote a rapid component (although not an increased extent) of PEG-triggered fusion between vesicles. Formation of an intervesicle SNARE complex was not required to see this effect.

6. At even higher surface concentration (1:250 for SX and 1:120 for SB), formation of an intervesicle SNARE complex promoted slow lipid mixing between vesicles in the absence of PEG at a rate comparable to earlier reports (17,21).

7. The ability of SNARE proteins to promote fusion pore formation is dependent on the presence of PS in the membranes used here.

These results lead us to several significant conclusions, which we now discuss.

SB and SX promote fusion of membranes juxtaposed by PEG

The principal effect of SB and SX is to promote formation of rapid stalk formation, but they also favor conversion of stalk to pore. It seems likely that the second effect is due to membrane disruption by the transmembrane portion of these proteins, although further work is needed to demonstrate this.

We have used PEG in this work to two ends. First, a low concentration of PEG (3 wt %) was used to aggregate vesicles and thereby promote intervesicle SNARE complex formation even at low copy numbers of SB (~4 or 8 per vesicle) and SX (~2 or 4). The probability of SNARE complex formation is presumably proportional to the probability of vesicle-vesicle collision (close contact) times the probability of SNARE complex assembly between contacting vesicles. Previous studies have used high copy numbers of SB and SX per vesicle to increase the second probability. This led to surface densities of proteins (0.015–0.08 per nm^2) considerably higher than we estimate for SB in purified synaptic vesicles (0.002 per nm^2 or 10–15 copies per synaptic vesicle). This estimate is derived from the total P/L ratio of 1:3 (wt/wt) for synaptic vesicles (30), the mean diameters of synaptic vesicles of 40–50 nm in the mammalian central nervous

system (31), the percentage of SB (~9%) to the total weight of protein content (32), an average molecular weight of 950 for the lipids, 387 for CH and 13,000 for SB, and an area per lipid of 0.65 nm^2. Our approach was to increase the probability of vesicle-vesicle contact so that we could follow fusion of vesicles joined by SNARE complex over a range of SX (0.0007–0.006 per nm^2) and SB (0.0016–0.012 per nm^2) surface densities that encompass the SB surface density that seems to exist in vivo but that also approaches the high surface densities previously examined.

Second, we have used PEG to trigger fusion between PEG-aggregated vesicles. This has allowed us to determine the effects of SNARE proteins on fusion independent of whether the SNARE complex was present to promote membrane contact. We have shown previously that a critical distance of membrane-membrane contact (~0.5 nm between headgroup phosphate groups) defines the critical PEG concentration at which fusion is first observed (5). We have performed all our PEG-mediated fusion experiments at the critical PEG concentration for control vesicles consisting of a synaptic vesicle-like mixture of lipids (DOPC/DOPE/SM/CH/DOPS at a 32:25:15:20:8 molar ratio) previously shown to optimize fusion versus leakage (4). To interpret results obtained under these conditions for SNARE-linked vesicles, we must first summarize what we know about PEG-mediated vesicle fusion.

PEG-mediated fusion is a three-step process involving two intermediates (3,33). The initial intermediate is termed a ''stalk'' (Fig. 9) and is marked by mixing of lipids between
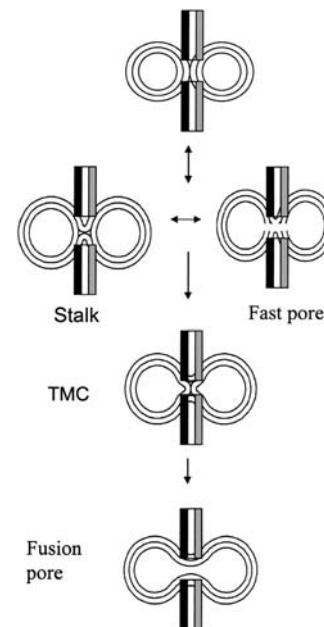

FIGURE 9 Cartoon summarizing the roles of SNAREs on PEG-mediated fusion of SB- and SX-containing SUVs. SX promotes stalk intermediate formation, fast pore formation in the stalk state, and evolution of the stalk intermediate to a fusion pore.

joined outer leaflet monolayers (hemifusion). If PEG is removed, this intermediate is reversible (3). A minimal and unstable pore can (but need not) appear in the stalk stage for both 45 nm (3) and 23 nm (15) vesicles. A larger pore appears more slowly and irreversibly late in the fusion process (3). Between the stalk and final fusion pore, a second intermediate irreversibly appears (transmembrane contact or TMC) (3). The kinetics of PEG-mediated fusion in every system we have studied (independent of lipid composition and vesicle size) can be fit by the same sequential, three-step process (contacting vesicles → stalk → TMC → pore) (G. Weinreb and B. R. Lentz, unpublished observations). Several parallels between this process and that detected in vivo have been noted, including an analogy between the two types of pores detected between vesicles and the 'flickering' pores and 'fusion' pores observed by patch-clamping exocytotic cells (33).

Experimentally, the fast and slow exponential components of contents mixing between 23 nm vesicles likely correspond to these two types of pores (15). The fast component has a small preexponential factor and roughly the same kinetic constant seen for fast lipid mixing. This seems to correspond to the transient, small pore associated with the initial hemifused intermediate in 45 nm-diameter vesicles (3). The slow contents-mixing event has a larger preexponential factor and probably represents the final and larger fusion pore (3,15). When two components of contents mixing are observed, two components of lipid mixing are also observed. In 23 nm vesicles, these probably correspond to lipid-mixing events associated with formation of the initial and second intermediates (15) (Weinreb and Lentz, unpublished observations). From this discussion of PEG-mediated fusion and our results, we conclude that SB and SX promote rapid formation of the stalk intermediate (along with a stalk-associated pore) and further promote conversion of the stalk to a final pore. Similar behavior was reported for both the transmembrane domain of Vesicular Stomatitis Virus G protein (34) and the fusion peptides of influenza virus hemagglutinin (4) and HIV gp41 (35). The ability of membrane-penetrating peptides to promote fusion was suggested to result, first, from their ability to destabilize the unfused bilayers and, second, from their ability to fill space and relieve the nonlamellar ''hydrophobic mismatch'' that inhibits evolution of the stalk toward a fusion pore (25). Our results suggest that the transmembrane regions of SX and SB might do the same.

SNAREs might promote stalk formation by 1), increasing the number of intervesicle contacts that can lead to stalks, 2), lowering the barrier to formation of the stalk intermediate by bringing membranes into close contact, 3), stabilizing the stalk relative to the initial state (contacting but unfused vesicles), or 4), raising the free energy barriers for either returning to the initial state or moving on to the TMC and pore. Since SNARE complexes hold membranes together (1), the first and second possibilities would at first thought seem most reasonable. However, the total extent of lipid mixing, which is a measure of the number of productive contacts per aggregate as well as the aggregate size (26), was not significantly different in the presence or absence of SNAREs. Since intact complex was not needed to see the effects of SX and SB, we do not need a SNARE complex that holds two membranes in close contact. These observations rule out the first and second possibilities. From Table 1, we see that SNARE complex promotes fusion pore formation, thus eliminating the fourth possibility, i.e., that SNAREs promote stalk formation by reducing the rate of conversion of the stalk to TMC or fusion pore (see Fig. 9). The possibility that SNAREs reduce the rate of return of stalk to initial state is also not likely, since the barrier for returning from the stalk to the initial state should be similar to that for forming a pore (36). This leaves the third possibility, namely that SNAREs promote stalk formation by raising the free energy of the unfused bilayers and/or lowering the free energy of the stalk. The transmembrane domain of Vesicular Stomatitis Virus G protein, which also promotes stalk formation, probably does so by destabilizing the unfused state (34) rather than by stabilizing the stalk. The transmembrane domains of SX and SB might do the same. The importance of the transmembrane domain is supported by two reports: first, that the transmembrane domains of SNAREs are also needed to induce lipid mixing between vesicles containing SNAREs at a high P/L ratio (22) and, second, that peptide mimics of SNARE transmembrane segments drive lipid mixing (37). Finally, both SX and SB promote leakage, with SX having the greater effect, also consistent with membrane packing disruption. In summary, it seems most likely that SB and SX promote stalk formation by disrupting and destabilizing the unfused state and may stabilize the TMC to promote conversion of stalk to a final pore. This latter possibility remains to be tested with synthetic transmembrane domain.

Membrane merger at high SNARE P/L ratio probably reflects the ability of SNARE proteins to disrupt membranes and promote stalk formation

The SNARE complex appears to have two roles in fusion. First, it brings membranes together. Several studies, including this one, have demonstrated this membrane-joining ability, and we have demonstrated that the complex we assemble between vesicles is the parallel complex expected in vivo (19). Since membrane contact is a prerequisite for fusion, the former effect is likely critical in the absence of PEG. However, we used PEG to aggregate vesicles and trigger fusion to reveal a second effect, namely that the SNARE proteins SB and SX promote rapid stalk and initial pore formation, probably due to disruption of the unfused membrane structure. In the absence of PEG and at a low copy number (≤4 per vesicle), we could detect no lipid or contents mixing between vesicles, even after assembly of intervesicle

SNARE complex in the presence of 3% PEG at 4°C (Figs. 5 and 6). However, at a high copy number (~20 per vesicle), slow lipid mixing was detected for such samples after incubating at 37°C (Fig. 7 *B*). QELS detected minimal growth in mean vesicle diameter in these samples, and both freeze-fracture (J. M. Costello, M. Dennison, M. Temgire, and B. R. Lentz; unpublished observations) and negative stain electron microscopy (17) showed somewhat larger vesicles having lamellar structures. Mixing of inner-leaflet components has also been reported under these conditions (21). These results make it clear that high copy numbers of SNARE complex trigger membrane merger. However, membrane merger does not demonstrate fusion unless membrane integrity is maintained. Merger can occur if two disrupted membranes come together and anneal. The fact that high SX copy numbers disrupt membrane integrity makes it impossible to demonstrate fusion by the accepted definition (''joining of both membrane and trapped aqueous compartments without significant loss of trapped contents'') and also makes it understandable how SX or SB might trigger merger.

Nonetheless, we can still ask what insight this in vitro observation might offer to the fusion process in vivo. In this regard, it is worth considering which role of the SNARE complex is responsible for this slow membrane merger. Does increased SNARE surface concentration lead to closer contact or to more membrane disruption? To address this, we compared the PEG-triggered fast rates of stalk formation (k_1 for lipid mixing) for double-reconstituted and quadruple-reconstituted vesicles joined by a stable SNARE complex (Table 2). These rates (corrected for the difference in endpoint calibration used in the BODIPY and Rh-PE/NBD-PE assays) were 0.17% saturation s^{-1} for double-reconstitution and 1.5% saturation s^{-1} for quadruple reconstitution. Single-reconstituted vesicles showed no fast rate of stalk formation (Table 1). It seems that adding increasing amounts of SB and/or SX to membranes increasingly disrupts membrane integrity and promotes stalk formation. This does not mean that higher SNARE copy numbers do not lead to SNARE complex oligomers that might favor closer membrane contact. They may, but the membrane-disrupting effects of SNARE proteins are sufficient to account for our results.

SN25 has little influence on fusion except to allow formation of a stable SNARE complex

Although SN25 is required to form a stable *trans* SNARE complex (Fig. 3 *C*), it had no effect on fusion (Table 1). This is consistent with the recent report that SN25 had little effect on docking efficiency or the probability of thermally induced fusion (16). It is also consistent with our finding that it is the presence of SX and/or SB in the membrane and not the formation of a tight complex (for which SN25 is required) that promotes fusion. This agrees with a recent report that SX in a planar bilayer alone is able to form a SNARE complex with

native v-SNARE of modified synaptic vesicles (38) or modified large dense-core neurosecretory granules (39).

Phosphatidylserine plays a previously unappreciated role in the SNARE-complex-mediated events associated with fusion

PS was needed in our vesicles to see the fusion-promoting effects of the SNAREs (Tables 1 and 3). Indeed, in the absence of PS, SNARE complex actually inhibited fusion but had no effect on formation of the initial stalk state (Table 3). This implies that at least one of the SNARE proteins interacts with PS in a way that alters either the protein or the membrane, or both. Since SN25 had no effect on PEG-mediated fusion, except when complexed with SX (Table 3), we conclude that it must be either SX or SB that interacts with PS. SX reconstituted into PS-containing supported bilayers has previously been noted to diffuse more slowly than it does in phosphatidylcholine bilayers (40). The molecular nature of the interaction of SX with PS is not known, but, given its role in promoting both stalk and pore formation (Table 1), this deserves examination.

Is SNARE complex the ''minimal machinery for cell membrane fusion''?

SX and SB, like the fusion peptides or transmembrane domains of viral fusion machines, have the ability to promote stalk and fusion pore formation. In addition, the intermembrane SNARE complex has the ability to bring membranes into contact, a prerequisite for fusion. However, SNARE-mediated membrane contact, even at very high P/L ratios, leads to an extremely slow rate of membrane merger, as compared either to PEG-mediated fusion between SB or SX vesicles or to the synaptic fusion process in vivo. It may be that SNARE proteins, because of other proteins present in the synaptic vesicle or the neuronal membrane, are more effective in promoting fusion in vivo than we have seen in our in vitro studies. This makes it likely that the SNARE-mediated events reported here and elsewhere, although useful for examining the mechanism by which SNAREs contribute to synaptic fusion, are not the controlling events in that process, and we must look elsewhere for the origin of the extremely fast fusion process seen at neuronal junctions.

REFERENCES

1. Sollner, T., S. W. Whiteheart, M. Brunner, H. Erdjument-Bromage, S. Geromanos, P. Tempst, and J. E. Rothman. 1993. SNAP receptors implicated in vesicle targeting and fusion. *Nature*. 362:318–324.

2. Chen, Y. A., and R. H. Scheller. 2001. SNARE-mediated membrane fusion. *Nat. Rev. Mol. Cell Biol.* 2:98–106.

3. Lee, J., and B. R. Lentz. 1997. Evolution of lipidic structures during model membrane fusion and the relation of this process to cell membrane fusion. *Biochemistry.* 36:6251–6259.

4. Haque, M. E., T. J. McIntosch, and B. R. Lentz. 2001. Influence of lipid composition on physical properties and PEG-mediated fusion of curved and uncurved model membrane vesicles: ''nature's own'' fusogenic lipid bilayer. *Biochemistry.* 40:4340–4348.

5. Burgess, S. W., T. J. McIntosh, and B. R. Lentz. 1992. Modulation of poly(ethylene glycol)-induced fusion by membrane hydration: importance of interbilayer separation. *Biochemistry.* 31:2653–2661.

6. Weninger, K., M. E. Bowen, S. Chu, and A. T. Brunger. 2003. Single-molecule studies of SNARE complex assembly reveal parallel and antiparallel configurations. *Proc. Natl. Acad. Sci. USA.* 100:14800–14805.

7. Bowen, M. E., D. M. Engelman, and A. T. Brunger. 2002. Mutational analysis of synaptobrevin transmembrane domain oligomerization. *Biochemistry.* 41:15861–15866.

8. Chen, P. S. J., T. Y. Toribara, and H. Warner. 1956. Microdetermination of phosphorus. *Anal. Chem.* 28:1756–1758.

9. Schwenk, E., and N. T. Werthesses. 1952. Studies on the biosynthesis of cholesterol. III. purification of cholesterol from perfusions of livers and other organs. *Arch. Biochem. Biophys.* 40:334–341.

10. Lentz, B. R., G. F. McIntyre, D. J. Parks, J. C. Yates, and D. Massenburg. 1992. Bilayer curvature and certain amphipaths promote poly(ethylene glycol)-induced fusion of dipalmitoylphosphatidylcholine unilamellar vesicles. *Biochemistry.* 31:2643–2653.

11. Wilschut, J., N. Duzgunes, R. Fraley, and D. Papahadjopoulos. 1980. Studies on the mechanism of membrane fusion: kinetics of calcium ion induced fusion of phosphatidylserine vesicles followed by a new assay for mixing of aqueous vesicle contents. *Biochemistry.* 19:6011–6021.

12. Talbot, W. A., L. X. Zheng, and B. R. Lentz. 1997. Acyl chain unsaturation and vesicle curvature alter outer leaflet packing and promote poly(ethylene glycol)-mediated membrane fusion. *Biochemistry.* 36:5827–5836.

13. Malinin, V. S., M. E. Haque, and B. R. Lentz. 2001. The rate of lipid transfer during fusion depends on the structure of fluorescence lipid probes: a new chain-labelled lipid transfer probe pair. *Biochemistry.* 40:8292–8299.

14. Wu, J. R., and B. R. Lentz. 1991. Mechanism of poly(ethylene glycol)-induced lipid transfer between phosphatidylcholine large unilamellar vesicles: a fluorescent probe study. *Biochemistry.* 30:6780–6787.

15. Evans, K. O., and B. R. Lentz. 2002. Kinetics of lipid rearrangements during poly(ethylene glycol)-mediated fusion of highly curved unilamellar vesicles. *Biochemistry.* 41:1241–1249.

16. Bowen, M. E., K. Weninger, A. T. Brunger, and S. Chu. 2004. Single molecule observation of liposome-bilayer fusion thermally induced by soluble N-ethyl maleimide sensitive-factor attachment protein receptors (SNAREs). *Biophys. J.* 87:3569–3584.

17. Schuette, C. G., K. Hatsuzawa, M. Margittai, A. Stein, D. Riedel, P. Kuster, M. Konig, C. Seidel, and R. Jahn. 2004. Determinants of liposome fusion mediated by synaptic SNARE proteins. *Proc. Natl. Acad. Sci. USA.* 101:2858–2863.

18. Fasshauer, D., H. Otto, W. K. Eliason, R. Jahn, and A. T. Brunger. 1997. Structural changes are associated with soluble N-ethylmaleimide-sensitive fusion protein attachment protein receptor complex formation. *J. Biol. Chem.* 272:28036–28041.

19. Sutton, R. B., D. Fasshauer, R. Jahn, and A. T. Brunger. 1998. Crystal structure of a SNARE complex involved in synaptic exocytosis at 2.4 Å resolution. *Nature.* 395:347–353.

20. Zenisek, D., J. A. Steyer, and W. Almers. 2000. Transport, capture and exocytosis of single synaptic vesicles at active zones. *Nature.* 406:849–854.

21. Weber, T., B. V. Zemelman, J. A. McNew, B. Westermann, M. Gmachl, F. Parlati, T. H. Sollner, and J. E. Rothman. 1998. SNAREpins: minimal machinery for membrane fusion. *Cell.* 92:759–772.

22. McNew, J. A., T. Weber, F. Parlati, R. J. Johnston, T. J. Melia, T. H. Sollner, and J. E. Rothman. 2000. Close is not enough: SNARE-dependent membrane fusion requires an active mechanism that transduces force to membrane anchors. *J. Cell Biol.* 150:105–117.

23. Parlati, F., T. Weber, J. A. McNew, B. Westermann, T. H. Sollner, and J. E. Rothman. 1999. Rapid and efficient fusion of phospholipid vesicles by the α-helical core of a SNARE complex in the absence of an N-terminal regulatory domain. *Proc. Natl. Acad. Sci. USA.* 96:12565–12570.

24. Tucker, W. C., T. Weber, and E. R. Chapman. 2004. Reconstitution of Ca2+-regulated membrane fusion by synaptotagmin and SNAREs. *Science.* 304:435–438.

25. Malinin, V. S., P. Frederik, and B. R. Lentz. 2002. osmotic and curvature stress affect PEG-induced fusion of lipid vesicles but not mixing of their lipids. *Biophys. J.* 82:2090–2100.

26. Wu, J. R., and B. R. Lentz. 1994. A method for quantitative interpretation of fluorescence detection of poly(ethylene glycol)-mediated 1-palmitoyl-2-[[[2-[4-(phenyl-*trans*-1,3,5-hexatrienly)phenyl]ethyl]oxyl]carbonyl]3-*sn*phosphatidylcholine (DPHpPC) transfer and fusion between phospholipid vesicles in the dehydrated state. *J. Fluoresc.* 4:153–163.

27. Deutsch, J. W., and R. B. Kelly. 1981. Lipids of synaptic vesicles: relevance to the mechanism of membrane fusion. *Biochemistry.* 20:378–385.

28. Finley, M. F., S. M. Patel, D. V. Madison, and R. H. Scheller. 2002. The core membrane fusion complex governs the probability of synaptic vesicle fusion but not transmitter release kinetics. *J. Neurosci.* 22:1266–1272.

29. Nickel, W., T. Weber, J. A. McNew, F. Parlati, T. H. Sollner, and J. E. Rothman. 1999. Content mixing and membrane integrity during membrane fusion driven by pairing of isolated v-SNAREs and t-SNAREs. *Proc. Natl. Acad. Sci. USA.* 96:12571–12576.

30. Benfenati, F., M. Bahler, R. Jahn, and P. Greengard. 1989. Interactions of synapsin I with small synaptic vesicles: distinct sites in synapsin I bind to vesicle phospholipids and vesicle proteins. *J. Cell Biol.* 108:1863–1872.

31. Jahn, R., and T. C. Sudhof. 1994. Synaptic vesicles and exocytosis. *Annu. Rev. Neurosci.* 17:219–246.

32. Walch-Solimena, C., J. Blasi, L. Edelmann, E. R. Chapman, G. F. Vonmollard, and R. Jahn. 1995. The t-SNAREs syntaxin-1 and SNAP-25 are present on organelles that participate in synaptic vesicle recycling. *J. Cell Biol.* 128:637–645.

33. Lee, J., and B. R. Lentz. 1998. Secretory and viral fusion may share mechanistic events with fusion between curved lipid bilayers. *Proc. Natl. Acad. Sci. USA.* 95:9274–9279.

34. Dennison, S. M., N. Greenfield, J. Lenard, and B. R. Lentz. 2002. VSV transmembrane domain (TMD) peptide promotes PEG-mediated fusion of liposomes in a conformationally sensitive fashion. *Biochemistry.* 41:14925–14934.

35. Haque, M. E., and B. R. Lentz. 2002. Influence of gp41 fusion peptide on the kinetics of poly(ethylene glycol)-mediated model membrane fusion. *Biochemistry.* 41:10866–10876.

36. Marrink, S. J., and D. P. Tieleman. 2002. Molecular dynamics simulation of spontaneous membrane fusion during a cubic-hexagonal phase transition. *Biophys. J.* 83:2386–2392.

37. Langosch, D., J. M. Crane, B. Brosig, A. Hellwig, L. K. Tamm, and J. Reed. 2001. Peptide mimics of SNARE transmembrane segments drive membrane fusion depending on their conformational plasticity. *J. Mol. Biol.* 311:709–721.

38. Woodbury, D. J., and K. Rognlien. 2000. The t-SNARE syntaxin is sufficient for spontaneous fusion of synaptic vesicles to planar membranes. *Cell Biol. Int.* 24:809–818.

39. McNally, J. M., D. J. Woodbury, and J. R. Lemos. 2004. syntaxin 1A drives fusion of large dense-core neurosecretory granules into a planar lipid bilayer. *Cell Biochem. Biophys.* 41:11–23.

40. Wagner, M. L., and L. K. Tamm. 2001. Reconstituted syntaxin1A/SNAP25 interacts with negatively charged lipids as measured by lateral diffusion in planar supported bilayers. *Biophys. J.* 81:266–275.